

Pamukkale Üniversitesi Mühendislik Bilimleri Dergisi





Compact Wideband Modified Wilkinson Filtering Power Divider with Wide Upper Stopband

Geniş Üst Durdurma Bantlı Kompakt Modifiye Edilmiş Geniş Bant Wilkinson Filtreleyen Güç Bölücü

Ali Kürşad Görür^{1*}, Ayyüce İlayda Bayrak², Alper Türkeli¹, Adnan Gorur²

¹Department of Electrical and Electronics Engineering, Nevşehir Hacı Bektaş Veli University, Nevşehir, Türkiy kgorur@nevsehir.edu.tr, alperturkeli@nevsehir.edu.tr

²Department of Electrical and Electronics Engineering, Niğde Ömer Halisdemir University, Niğde, Türkiye. ayyuceilaydaa@gmail.com, adnangorur@hotmail.com

Received/Geliş Tarihi: 02.07.2025 Accepted/Kabul Tarihi: 13.10.2025 Revision/Düzeltme Tarihi: 08.10.2025 doi: 10.65206/pajes.60206 Research Article/Araştırma Makalesi

Öz

A compact wideband modified Wilkinson-type filtering power divider (MWFPD) with wide stopband is presented. The MWFPD is developed by cascading a modified Wilkinson power divider (MWPD) and a filtering section constituting stepped-impedance resonator (SIR)-loaded three-coupled lines (TCLs). The arms of the MWPD also consist of SIRs. By suppressing harmonics using a single open stub at the input port only, the upper stopband is extended up to 20 GHz with 20 dB rejection. The designed MWFPD has also been fabricated to verify the mathematical and electromagnetic simulation results. The measured results exhibit an excellent agreement with the predicted results. The center frequency of the fabricated circuit has been measured at 4.36 GHz with a fractional bandwidth (FBW) of 44 %. The proposed MWFPD not only exhibits competitive performance but also provides ease of fabrication and desian.

Anahtar kelimeler: Filtering power divider, modified Wilkinson power divider, wide stopband.

1 Introduction

²With the ever-increasing demands of modern wireless communication systems, filtering power dividers (FPDs) with wideband harmonic suppression are developed rapidly. In this context, the growing variety of FPD topologies still needs further development to incorporate different filtering characteristics, such as wide passband/stopband, high rejection, high isolation, low insertion loss and reduced size [1][14]. To date, many techniques have been used to design compact FPDs with wide stopband [2]-[10].

To achieve wide stopband goal, the FPD designs in the relevant literature have been generally based on microstrip structures with short-circuited stubs [2], discriminating coupling [3], stepped-impedance coupled lines [4], dual-resonance (DRRs) and spur lines [5], microstrip/defected ground structure (HMS/DGS) [6], [7], the substrate integrated DGS (SIDGS) [8], HMS/SIDGS [9] and lumped elements [10]. Furthermore, the structures based on SIDGS, hybrid MS/SIDGS, and lumped elements are also composed of multiple layers. All of the designs mentioned above require extra manufacturing processes and costs. On the

Geniş durdurma bandına sahip konpakt geniş bantlı modifiye edilmiş Wilkinson tipi filtrelem zgüç böl icü (MWFPD) sunulmaktadır. MWFPD, modifiye edilmiş hi Mukinson güç bölücü (MWPD) ve basamak empedans rezona örü (SİK) yüklü üç kuplajlı hatlardan (TCL) oluşan bir filtreleme bölü münün kaskat bağlanmasıyla geliştirilmiştir. MWPD'nin kolları da SİK lera in oluşmaktadır. Sadece giriş portunda tek bir açık devre sonı ndurma asaplama kullanılmasıyla harmonikler bastırılarak üst du duşma bindı 20 dB reddetme ile 20 GHz'e kadar uzatılmaktadır. Tasa danan MWFPD ayrıca matematiksel ve elektromanyetik simüla von sonuçlarını doğrulamak için imal edilmiştir. Ölçülen sonuçlar öngörülen sonuçlarla mükemmel bir uyum göstermektedir. Üretilen devrenin merkez frekansı %44'lük kısmi bant genişliği (FBW) ile 4.36 GHz'de ölçülmüştür. Önerilen MWFPD sadece rekabetçi bir performans sergilemekle kalmayıp aynı zamanda üretim ve tasarım kolaylığı da sunmaktadır.

Keywords: Filtreleyen Güç Bölücü, modifiye edilmiş Wilkinson güç bölücü, geniş durdurma bandı.

other hand, the common feature of the FPD designs in the literature, except for studies in [11]-[13], is that they use topologies consisting of the two-way double resonators. Consequently, such topologies always lead to a relatively larger occupied area, high-losses, and even complex design.

This paper introduces a modified Wilkinson FPD (MWFPD) with a stepped impedance resonator (SIR) filtering section. The proposed FPD uses a Wilkinson power divider (WPD) for power splitting and a SIR-loaded three-coupled lines (TCLs) for wideband filtering. As is well-known, two filtering sections are generally integrated into each branch of the PD, which leads to an increase in circuit size and transmission loss. By using only one filtering section at the input port instead of the two-way double resonators, both circuit size and loss are reduced. In addition, to reduce the circuit size, each branch of the MWFPD is also constructed from a stepped-impedance transmission line, unlike the conventional WPD. Moreover, to suppress the harmonic signal in the upper stopband and thus achieve a wider upper stopband, a single open stub is connected at the input port to create a transmission zero at the harmonic frequency. As a result, a novel, compact, and low-loss wideband FPD topology with a stopband extended up to 20 GHz, good in-band

Abetract

^{*}Corresponding author/Yazışılan Yazar

^{*}Yazışılan yazar/Corresponding author

isolation, and high rejection characteristics is presented. The proposed wideband FPD was designed, implemented, and tested for demonstration. The measured results exhibit excellent agreement with the simulated ones.

2 Design Procedure

The layout of the proposed FPD with wide stopband is shown in Fig. 1a. Essentially, a modified Wilkinson power divider (MWPD) and a single filtering section are cascaded. The arms of the MWPD consist of stepped-impedance resonators (SIRs). The SIR increases the selectivity by highlighting one of the poles that tend to disappear due to the cascade of the PD section and the filtering section, and also contributes to the reduction of the circuit size, albeit slightly. Meanwhile, an isolation resistor is connected between the two output lines for achieving a good in-band isolation level. It should be noted that although SIRs are used instead of the uniform impedance resonators (UIRs) of the classical WPD, the value of the isolation resistor R has not been changed. The filtering section consists of a SIR loaded TCLs, which has three transmission poles in the passband and two transmission zeros the band edges. In addition, a single open stub is used at the input port to extend the upper stop band up to 20 GHz. However, it should be noted that the open stub is not included in the following analyses for simplicity.

Filtering Response

The even-mode equivalent circuit with the left side excitation can be used for transmission properties as shown in Fig. 1b. The input impedance at port 1 in the figure can be calculated as follows:

$$Z_{1in} = Z_1 \frac{Z_{ic} + jZ_1 \tan \theta_a}{Z_1 + jZ_{ic} \tan \theta_a}$$
 (1)

with

$$Z_{ic} = Z_{11} - \frac{Z_{13}^2}{Z_{ia} + Z_{11}} + P \cdot \left(1 - \frac{Z_{13}}{Z_{ia} + Z_{11}}\right) Z_{15}$$
 (2)

$$P = \frac{(Z_{ia} + Z_{11})Z_{15} - Z_{13}Z_{15}}{Z_{15}^2 - (Z_{ia} + Z_{11})(Z_L + Z_{55})}$$
(3)

$$Z_{ia} = Z_1 \frac{Z_{i3} + jZ_{i1} \tan \theta_a}{2Z_1 + jZ_{i3} \tan \theta_a}$$
 (4)

$$Z_{i3} = Z_3 \frac{Z_{i4} + j Z_3 \tan \theta_3}{Z_3 + j Z_{i4} \tan \theta_3}$$
 (5)

$$Z_{14} = Z_4 \frac{Z_0 + jZ_4 \tan \theta_4}{Z_4 + jZ_0 \tan \theta_4} \tag{6}$$

$$Z_{15}^{2} - (Z_{ia} + Z_{11})(Z_{L} + Z_{55})$$

$$Z_{ia} = Z_{1} \frac{Z_{i3} + jZZ_{1} \tan \theta_{a}}{2Z_{1} + jZ_{i3} \tan \theta_{a}}$$

$$Z_{i3} = Z_{2} \frac{Z_{i4} + jZ_{3} \tan \theta_{3}}{Z_{3} + jZ_{i4} \tan \theta_{3}}$$

$$Z_{i4} = Z_{4} \frac{Z_{0} + jZ_{4} \tan \theta_{4}}{Z_{4} + jZ_{0} \tan \theta_{4}}$$

$$Z_{L} = JZ_{1} \frac{Z_{1} \tan \theta_{b} - Z_{2} \cot \theta_{2}}{Z_{1} + Z_{2} \tan \theta_{b} \cot \theta_{2}}$$
(7)

 $(m, n = 1, 2, \dots 6)$ is the impedance matrix elements of the TCLs denoted and according to approximation in [15] can be determined as

$$Z_{11} = Z_{33} = -j \frac{1}{q+2} \left(Z_{ee} + \frac{q}{2} Z_{oo} + \frac{q+2}{2} Z_{oe} \right) \cot \theta_c$$
 (8)

$$Z_{13} = -j\frac{1}{q+2} \left(Z_{ee} + \frac{q}{2} Z_{oo} - \frac{q+2}{2} Z_{oe} \right) \cot \theta_c \tag{9}$$

$$Z_{15} = -j \frac{\sqrt{q}}{q+2} (Z_{ee} - Z_{oo}) \csc \theta_c$$
 (10)

$$Z_{55} = -j\frac{1}{q+2}(qZ_{ee} + 2Z_{oo})\cot\theta_c \tag{11}$$

with

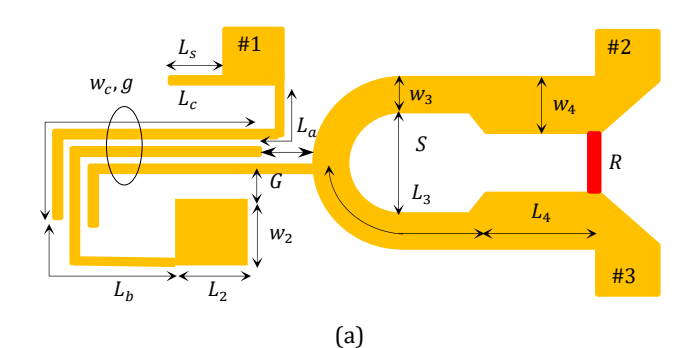
$$q = \frac{2(Z_{ee} - Z_{oo})^2 - Z_{oe}(Z_{oe} - Z_{ee} - Z_{oo}) - Z_{ee}Z_{oo}}{2Z_{ee} - Z_{oo} - Z_{oe}}$$
(12)

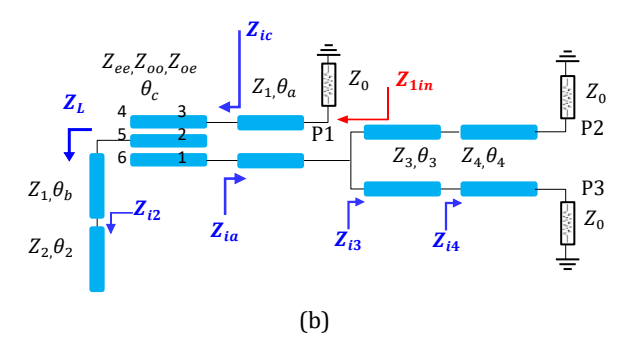
In (8)-(12), the impedances Z_{ee} , Z_{oo} and Z_{oe} are even-even, odd-odd and odd-even mode characteristic impedances of each coupled line constituting the TCLs. Their widths and the gaps between them are w_c and g, respectively, as shown in Fig. 1a. The electrical lengths of the TCLs are denoted as θ_c . So, the transmission properties of the proposed FPD determined by the scattering parameters given as

$$S_{11} = \frac{Z_{1in} - Z_0}{Z_{1in} + Z_0} \tag{13}$$

$$|S_{21}| = |S_{31}| = \frac{1 - |S_{11}|^2}{2} \tag{14}$$

In this study, a compact wideband FPD operating at 3.4-5.3~GHzwith 20-dB RL is designed. The substrate used in this study is Rogers RT5870 with a relative dielectric constant of 2.33 and a thickness of 0.787 mm. Since the return loss (RL) within the passband is chosen to be greater than 20 dB, the relevant impedances and electrical lengths can be determined by optimizing the input impedance Z_{1in} . The mode impedances of the TCLs are obtained as $Z_{ee} = 310 \Omega$, $Z_{oo} = 127 \Omega$ and $Z_{oe} = 155 \Omega$. The characteristic impedances of the line sections and open stubs in Fig. 1 are calculated as $Z_1 = 155 \,\Omega$, $Z_2 = 40 \,\Omega$, $Z_3 = 70.2 \,\Omega$, and $Z_4 = 50 \,\Omega$. The electrical lengths of the lines are obtained as $\theta_a = 10.7^0$, $\theta_b = 35.5^0$, $\theta_c = 82.2^0$, $\theta_2 = 32.56^0$, $\theta_3 = 90^0$ and $\theta_4 = 0.37^0$. The filtering response calculated through the above analysis is shown in Fig. 2.





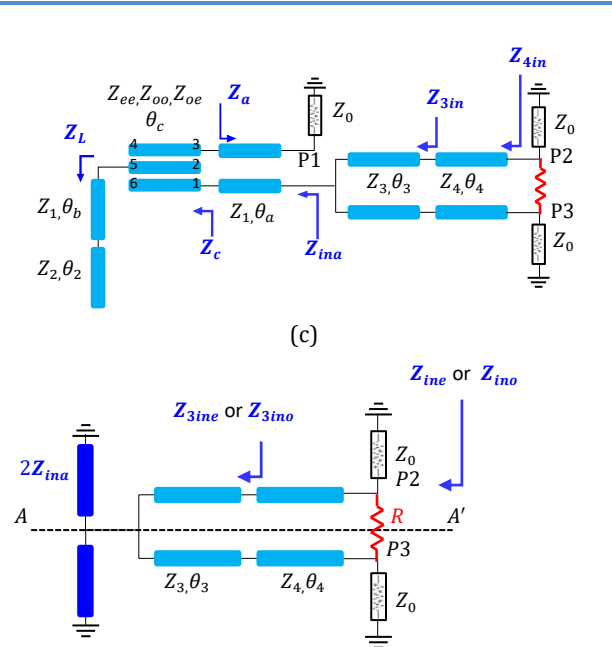


Figure 1. (a) Layout of the proposed wideband MWFPD, (b) equivalent transmission line circuit with input port-side excitation (even-mode equivalent circuit for $R=\infty$), (c) output port-side excitation and (d) simplified circuit derived from the circuit in (c).

(d)

2.2 Isolation Response

By applying even-odd mode analysis to the simplified equivalent circuit in Fig. 1d, which is derived from the odd mode equivalent circuit in Fig. 1c, the isolation parameter S_{32} of the proposed FPD can be calculated as

$$S_{32} = \frac{(Z_{ine} - Z_{ino})Z_0}{(Z_0 + Z_{ine})(Z_0 + Z_{ino})}$$
(15)

where the odd- and even-mode input impedances at port 2 (or 3), respectively, can be determined as

$$Z_{ino} = \frac{Z_{4ino} \cdot R}{2Z_{4ino} + R} \tag{16}$$

with

$$Z_{4ino} = jZ_4 \frac{Z_3 \tan \theta_3 + Z_4 \tan \theta_4}{Z_4 - Z_3 \tan \theta_3 \tan \theta_4}$$
 (17)

and

$$Z_{ine} = Z_4 \frac{Z_{3ine} + jZ_4 \tan \theta_4}{Z_4 + jZ_{3ine} \tan \theta_4}$$
 (18)

with

$$Z_{3ine} = Z_3 \frac{2Z_{ina} + jZ_3 \tan \theta_3}{Z_3 + j2Z_{ina} \tan \theta_3}$$
 (19)

$$Z_{ina} = Z_1 \frac{Z_c + jZ_1 \tan \theta_a}{Z_1 + jZ_c \tan \theta_a}$$
(20)

$$Z_c = Z_{11} - \frac{Z_{13}^2}{Z_a + Z_{11}} + Q \cdot \left(1 - \frac{Z_{13}}{Z_a + Z_{11}}\right) Z_{15}$$
 (21)

$$Q = \frac{(Z_a + Z_{11})Z_{15} - Z_{13}Z_{15}}{Z_{15}^2 - (Z_a + Z_{11})(Z_L + Z_{55})}$$
(22)

$$Z_a = Z_1 \frac{Z_0 + jZ_1 \tan \theta_a}{Z_1 + jZ_0 \tan \theta_a}$$
 (23)

The isolation response calculated through the above analysis is shown in Fig. 2.

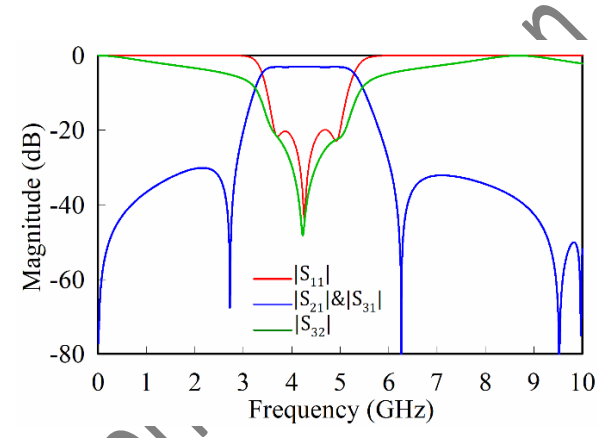


Figure 2. Calculated S-parameters

3 Implementation, Results and Discussion

Based on the abovementioned analysis, an MWFPD operating at 4.35 GHz with 3-dB FBW of 44% and 20-dB RL is designed and implemented on a Rogers RT5870 substrate with a relative dielectric constant of 2.33 and a thickness of 0.787 mm. The characteristic impedance of the section with the length L₃ of the PD is fixed to $\sqrt{2}Z_0$, as in the conventional WPD, while the characteristic impedance and electrical length of the length L₄ are modified and optimized by full-wave EM simulations. Thus, the size of the PD section is slightly reduced. However, the value of the isolation resistor is fixed at 100 Ω , as in conventional WPDs, for convenience. On the other hand, a quarter wavelength open stub is placed at the input port of the MWFPD to suppress the harmonic observed around 17 GHz, as shown in Fig. 3. The simulation model is depicted in the inset of the figure. As can be seen, the proposed MWFPD exhibited wide stopband with an insertion loss of larger than 19.3 dB over a wide frequency range up to 14.9 GHz, due to its filtering section consisting of SIR loaded TCLs. By adding an open stub at the input port, the upper stopband with 19 dB-rejection level is extended up to 20 GHz.

The final dimensions of the proposed WB-BPF can be determined through full-wave EM simulations performed using Sonnet Software. The optimized final dimensions of the proposed MWFPD with wide stopband are determined as La=2.4 mm, Lb=5.5 mm, Lb=11 mm, L2=3.7 mm, L3=9.85 mm, L4=4.1 mm, and Ls=2.15 mm. The value of the isolation resistor is fixed at 100 Ω , for convenience. The implemented circuit has a total size of 7.4 mm×24.65 mm $(0.15\lambda_g \times 0.5\lambda_g = 0.075\lambda_g^2)$. Photograph of the fabricated FPD is illustrated in the inset of Fig. 4a.

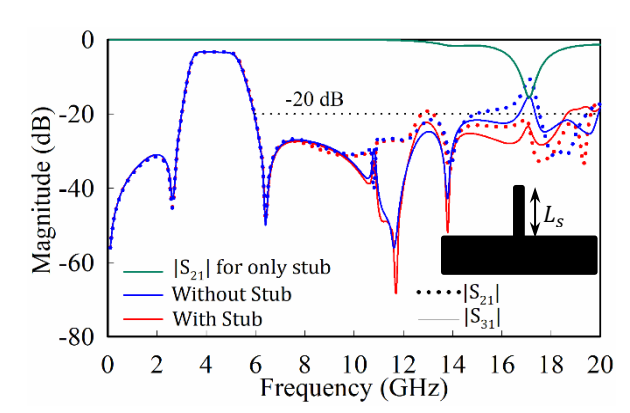


Figure 3. The simulated S_{21} parameters of the proposed FPD with and without open stub, and the open stub used for harmonic suppression.

The simulated and measured frequency responses of the proposed compact FPD with wide stopband are depicted in Fig. 4a in a good agreement. The measurements were performed by Keysight N5222A PNA Network Analyzer. The measured center frequency and 3-dB FBW are 4.36 GHz and 44%. The minimum insertion loss was less than 0.4 dB in the measurements and the return loss is better than 20 dB. The measured transmission response achieves 20 dB-rejection level up to 20 GHz. The measured amplitude and phase imbalances between the two outputs are 0.26 dB and 1.8°, respectively, as shown in Fig. 4b. The measured in-band isolation is greater than 21.4 dB. The matching performances of $|S_{22}|$ and $|S_{33}|$ are also measured around 20 dB, as shown in Fig.4c.

Finally, the comparison of the proposed wideband FPD with the circuits exhibiting similar properties is shown in Table 1. As it can be seen from the table, the proposed wideband FPD exhibits not only compact size and wide stopband but also a good isolation and low insertion loss. In addition, due to the single-sided microstrip structure, the proposed MWFPD provides the advantage of fabrication simplicity.

Table 1. Comparison with previous FPDs with wide stopband.

Ref.	f ₀ GHz	FBW (%)	IL (dB)	I (dB)	Size λ_g^2	Stopband Rejection	Tech
2	1	43	3.2	20	0.146	to 3.9 GHz 20 dB	CSL
3	1.4	15	1.3	>16	0.025	to 8.5 GHz 30 dB	CSL
4	2.02	49.5	NA	22	0.051	to 9.36 GHz 40 dB	CSL
7	2.31	17.7	1.2	>17	0.38	to 20 GHz 30 dB	DS
8	2.87	23	1	>20	0.10	to 25 GHz 28 dB	ML
9	5.4	74	0.74	19	0.136	to 40 GHz 19 dB	ML
This work	4.36	44	0.4	21.4	0.075	to 20 GHz 20 dB	SSMS

FBW: Fractional Bandwidth, IL: Insertion Loss, I: In-band Isolation, Tech: Technology, CSL: Contains shorted line, DS: Double-sided, ML: Multi-layer, SSMS: Single-sided microstrip.

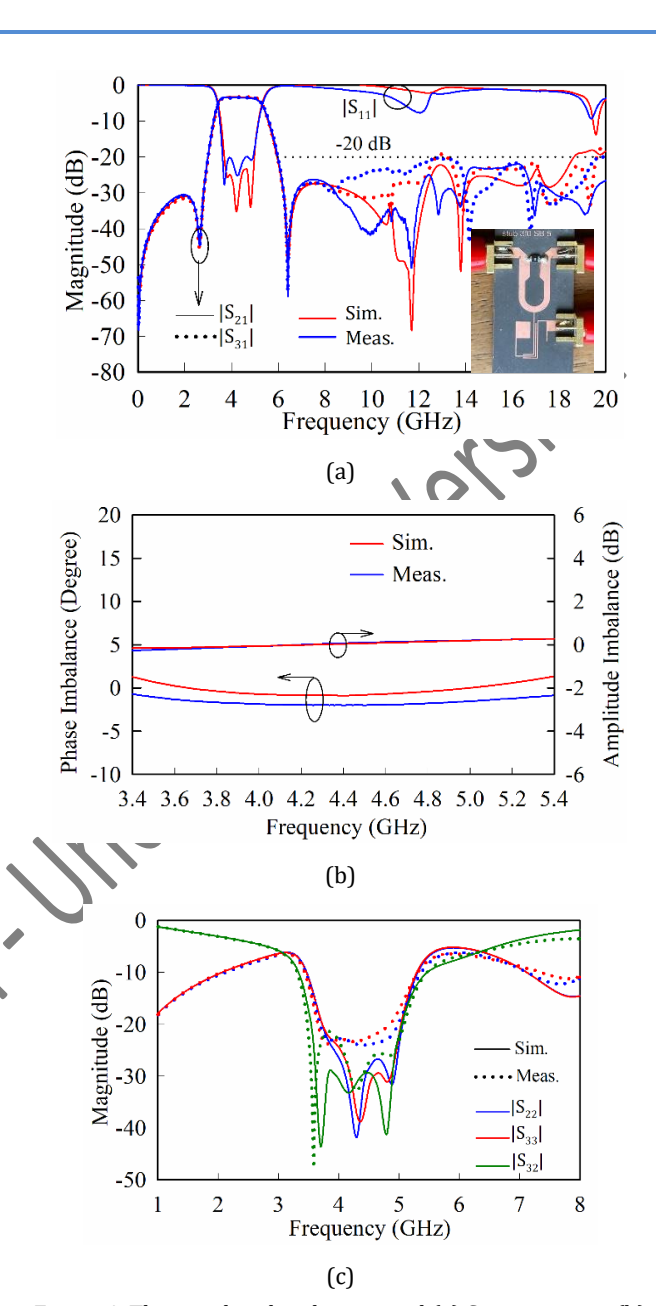


Figure 4. The simulated and measured (a) S-parameters, (b) phase and amplitude imbalance and (c) isolation and matching performance of the proposed wideband FPD with wide stopband.

4 Conclusions

By cascading a modified WPD with only one single filtering section consisting of well-designed SIR loaded TCLs, a new wideband MWFPD has been developed with wide stopband, compact size, good isolation, and low-loss. By suppressing harmonics using a single open stub at the input port only, the stopband has been extended with 20 dB rejection out to 20 GHz. The proposed MWFPD not only exhibits competitive performance but also provides fabrication and design simplicity.

As a future work, it is expected that the proposed approach will be used to construct a MIMO filtenna for sub-6 GHz 5G applications. The MIMO filtenna to be developed is going to be consisted of a wideband filter and a monopole antenna. The wideband filter proposed here will be useful for the design

methodology of this filtenna. It is also planned to insert a controllable notch band in the frequency region of sub-6 GHz, especially to cover the frequency range of between 5.5 and 5.8 GHz.

The FPDs not only have similar application areas with conventional power dividers, but also have the advantages of exhibiting filtering characteristics. Therefore, there is no need for an additional filter structure. On the other hand, it is well known that the power dividers can be used to feed antenna networks, phase shifters and power amplifiers. They also play a critical role in communication systems such as phased arrays, transceivers, antenna front-end systems and Internet of Things (IoT) applications.

5 Acknowledgement

6 Author Contribution Statement

All authors contributed to all stages of the mathematical, simulation and experimental work of the article.

7 Ethics committee approval and conflict of interest statement

"There is no need for ethics committee approval for the prepared article."

"There is no conflict of interest with any person/institution in the prepared article."

8 References

- [1] Tian H, Xiao L, Yu H, Chen Y, Shi L, Xiao F. "Wideband Microstrip Filtering Power Divider Designed by Direct Synthesis Technique (DST)". *IEEE Microwave and Wireless Components Letters*, 32(6), 507-510, 2022
- [2] Wu Y, Zhuang Z, Liu Y, Deng L and Ghassemlooy Z. "Wideband Filtering Power Divider With Ultra-Wideband Harmonic Suppression and Isolation". *IEEE Access*, 4, 6876-6882, 2016.
- [3] Zhao X-L, Gao L, Zhang XY and Xu J-X. "Novel Filtering Power Divider With Wide Stopband Using Discriminating Coupling". *IEEE Microwave and Wireless Components Letters*, 26(8), 580-582, 2016.
- [4] Chen M-T and Tang C-W. "Design of the Filtering Power Divider With a Wide Passband and Stopband". *IEEE Microwave and Wireless Components Letters*, 28(7), 570-572, 2018.
- [5] Wen P, Ma Z, Liu H, Zhu S, Ren B, Song Y, Wang X and Ohira M. "Dual-Band Filtering Power Divider Using Dual-Resonance Resonators With Ultrawide Stopband and Good Isolation". *IEEE Microwave and Wireless Components Letters*, 29(2), 101-103, 2019.
- [6] Rao Y, Qian HJ, Yang B, Gomez-Garcia R and Luo X. "Dual-Band Bandpass Filter and Filtering Power Divider With Ultra-Wide Upper Stopband Using Hybrid Microstrip/DGS Dual-Resonance Cells". IEEE Access, 8, 23624-23637, 2020.
- [7] Fan L, Qian HJ, Yang B, Wang G and Luo X. "Filtering Power Divider with Wide Stopband Using Open-Stub Loaded

- Coupled-Line and Hybrid Microstrip T-Stub/DGS Cell". 2018 IEEE MTT-S International Microwave Symposium, PA, USA, 10-15 June 2018.
- [8] Han C, Tang D, Deng Z, Qian HJ and Luo X. "Filtering Power Divider With Ultrawide Stopband and Wideband Low Radiation Loss Using Substrate Integrated Defected Ground Structure". IEEE Microwave and Wireless Components Letters, 31(2), 113-116, 2021.
- [9] He Z and Luo X. "A 3.4-7.4-GHz Filtering Power Divider With Wide Stopband and Low Radiation Loss Using Triple-Mode Hybrid Microstrip/SIDGS Resonator" 2024 54th European Microwave Conference (EuMC), Paris, France, 24-26 September 2024.
- [10] Liu Z-H, Zhou Y-J and Cheng C-H. "A Miniaturized Filtering Power Divider With High Selectivity and Wide Stopband Based on 3-D Heterogeneous Integration Technology". IEEE Transactions on Circuits and Systems II: Express Briefs, 71(6), 2951-2955, 2024.
- Briefs, 71(6), 2951-2955, 2024.
 [11] Zhang G, Wang X and Yang J. "Dual-band microstrip filtering power divider based on one single multimode resonator". *IEEE Microwave and Wireless Components Letters*, 28(10), 891-893, 2018.
- [12] Zhang G, Wang X, Hong J-S and Yang J. "A High-Performance Dual-Mode Filtering Power Divider With Simple Layout". *IEEE Microwave and Wireless Components* Letters, 28(2), 120-122, 2018.
- [13] Zhang Q, Zhang G, Liu Z, Chen W and Tang W. "Dual-band filtering power divider based on a single circular patch resonator with improved bandwidths and good isolation". IEEE Transactions on Circuits and Systems II: Express Briefs, 68(11), 3411–3415, 2021.
- [14] Cakır M and Karpuz C. "Two and four-way Wilkinson power divider with slow-wave microstrip structures". Pamukkale University Journal of Engineering Sciences, 2025.
- [15] Pavlidis D and Hartnagel HL. "The design and performance of three-line microstrip couplers". *IEEE Transactions on Microwave Theory and Techniques*, 24(10), 631–640, 1976.